

Single-Pixel IQ Monitor via Computational Coherent Reception with Widely Linear Phase Retrieval

Yuki Yoshida⁽¹⁾, Takahito Tanimura^(2,*), Setsuo Yoshida⁽²⁾, Takeshi Hoshida⁽²⁾, Naokatsu Yamamoto⁽¹⁾

⁽¹⁾ National Institute of Information and Communications Technology (NICT), 4-2-1 Nukui-kitamachi, Koganei, Tokyo, Japan, yuki@nict.go.jp

⁽²⁾ Fujitsu Limited, 1-1 Shin-ogura, Saiwai-ku, Kawasaki, Japan, hoshida@fujitsu.com

(*: currently with Hitachi Ltd.)

Abstract For in-service and in-field monitoring of frequency-dependent IQ imbalance in optical IQ modulators, we propose a low-complexity IQ monitor using a single photodetector based on phase retrieval. The feasibility of the proposed single-pixel IQ monitor was demonstrated experimentally with a 63.25-Gbaud 16QAM signal.

Introduction

In modern fiber-optic communication systems, recently, symbol rate and modulation order of optical signal have been rapidly increased, e.g. 100 Gbaud and 16QAM. Thus, more precise monitoring and calibration techniques for an imperfection of the transceivers, such as mismatches between In-phase (I) and Quadrature (Q) tributaries of optical IQ modulators, namely IQ imbalance (IQI), become essential to achieve longer transmission distance and higher capacity^[1,2]. A slight imbalance of timing, phase, and/or amplitude between the IQ branches severely can hurt higher-order and higher symbol rate signal^[3,4]. Particularly, frequency-dependence of the imbalances, called frequency-dependent IQI (FD-IQI), can represent the most stringent limitations^[5]. The IQ impairments must keep within such tight penalty limits over wavelength and temperature during product lifetime. Thus, not only a factory calibration, but also a continued monitoring and calibration during service in field becomes increasingly important^[6-8].

For the factory calibration, IQI is often monitored by using a bulky measurement instrument, namely a “gold-standard” coherent receiver. This monitoring technique is applicable for the in-service in-field monitoring if it is implemented with the far-end coherent receiver^[1,8-14]. However, such coherent-based IQ monitoring (Coh-IQM) requires the advanced DSP for separating transmitter IQI from receiver IQI, carrier frequency offset (CFO), and other transmission impairments in practice^[1,8,12,14]. Additionally, a feedback path is necessary for transmitter calibration.

On the other hand, some low-cost IQ monitors based on direct-detection (DD-IQM) have been proposed and demonstrated mainly for in-field calibration of pluggable optics^[6,7,15-18]. DD-IQMs are low complexity and often integrable with the transmitter. However, in order to separately

monitor the IQ components based on direct detection, a specific pilot tone or dither signal needs to be sent in most cases. The use of the pilot tone limits their application in the in-service scenario; Even a small dither signal may be harmful for extremely high-order and symbol rate modulation formats. In addition, most conventional DD-IQMs pertain to the frequency-independent IQI model^[7,15,17]. As far as the authors know, few works have been reported on the in-service and in-field IQM, which can fully characterize FD-IQI, based on direct detection.

In this work, we propose a DD-IQM for FD-IQI based on the idea of phase retrieval (PR)^[19], called single-pixel IQ monitor (SP-IQM). Complex-valued impulse responses of the individual IQ tributaries are computationally retrieved from the phase-less measurements of the information-bearing signal by a novel widely-linear (WL) PR technique. Specific tone or dither signal is not needed. We show the feasibility of the proposed SP-IQM experimentally in a 63.25-Gbaud 16QAM signal.

FD-IQI Estimation based on DD via WL-PR

The schematic architecture of the proposed SP-IQM is shown in Fig. 1. The monitor consists of a single photodetector (PD) and an analog-to-digital converter (ADC). Suppose the driving signal is limited to the linear region, the baseband equivalent of the IQ modulator output $E(t) \in \mathbb{C}$ under FD-IQI is given by the WL model^[20,21]

$$E(t) \propto E_0 \{ h_+(t) * s(t) + h_-(t) * s^*(t) + \delta \}, \quad (1)$$

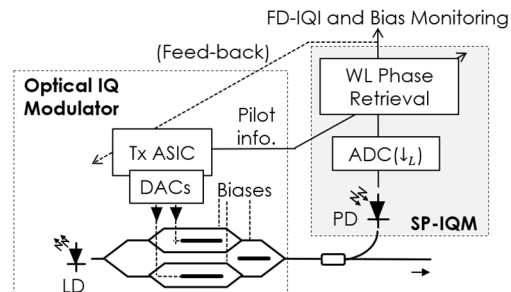


Fig. 1: Schematic architecture of PR-based SP-IQM

where $E_0 \in \mathbb{C}$ is the optical carrier, $*$ denotes linear convolution, $(\cdot)^*$ is complex conjugation, and $s(t) \in \mathbb{C}$ is the driving (baseband) signal. The response of the modulator is represented by two FIR filters $h_{+/-}(t) \in \mathbb{C}^L$, which can be parameterized by $h_{+/-}(t) = \{h_I(t) \pm (1 + \epsilon)h_Q e^{j\theta}\}/2$. Here, $h_{I/Q}(t)$ is the overall response of the I/Q tributary including such as DAC, driver, pluggable connector, and PCB trace. $\epsilon/\theta \in \mathbb{R}$ denote the frequency-independent power/phase mismatch. The DC offset $\delta := \delta_I + j(1 + \epsilon)\delta_Q e^{j\theta}$, where $\delta_{I/Q} \in \mathbb{R}$ is the DC-bias skew at the I/Q branch. The relative difference between $h_I(t)$ and $h_Q(t)$ makes IQI frequency selective.

SP-IQM obtains $h_{+/-}(t)$ and δ from the phaseless measurement $|E(t)|^2$. The most of the conventional IQMs estimate the frequency-independent IQI, i.e., $\{\epsilon, \theta, \delta\}$, parametrically by assuming $h_I(t) = h_Q(t)$ (or $h_Q(t - \tau)$). Moreover, $s(t)$ often needs to be a specific tone or dither signal. This limits the application of the IQMs in the in-field and in-service scenarios. Here, we propose to estimate the FD-IQI, i.e., $\{h_{+/-}(t), \delta\}$, directly by means of PR based on the information-bearing and thus random signal $s(t)$.

Suppose the monitor PD and the ADC are ideal. The PD output after the sampling is given by

$$\psi = |\mathbf{h}_+^\top \mathbf{s} + \mathbf{h}_-^\top \mathbf{s}^* + \delta \mathbf{1}|^2, \quad (2)$$

where $\mathbf{h}_{+/-} \in \mathbb{C}^{L \times 1}$ (here L is the delay spread of $h_{+/-}(t)$ in the sample domain.) and $\mathbf{s} \in \mathbb{C}^{L \times 1}$ are the discrete-time equivalents of $h_{+/-}(t)$ and $s(t)$, respectively. $\mathbf{1}$ denotes the $L \times 1$ all-ones vector and $(\cdot)^\top$ stands for transpose. Similar to [22], we consider sending K independent pilot signal blocks $\mathbf{s}_k \in \mathbb{C}^{L \times 1} (k = 1, \dots, K)$. Then, the estimation of $\mathbf{h}_{+/-}$ in (2) can be formulated by

$$\text{find } \bar{\mathbf{h}} \text{ s.t. } \psi_k = |\bar{\mathbf{s}}_k^\top \bar{\mathbf{h}}|^2 \quad (k = 1, \dots, K), \quad (3)$$

for given $\{\bar{\mathbf{s}}_k\}$. Here, $\bar{\mathbf{h}} := [\mathbf{h}_+^\top, \mathbf{h}_-^\top, \delta]^\top \in \mathbb{C}^{(2L+1) \times 1}$, and $\bar{\mathbf{s}}_k := [\mathbf{s}_k^\top, \mathbf{s}_k^H, 1]^\top \in \mathbb{C}^{(2L+1) \times 1}$ ($(\cdot)^H$ is the Hermitian transpose). The WL channel and bias estimation in (2) is successfully cast into the common form of *phase retrieval* [19]. The problem of PR arises in many areas such as crystallography and diffraction imaging. In the last decade, substantial progress has been made in

PR based on the theoretical connections with algebraic geometry and compressed sensing.

Firstly, it is conjectured that $4N - 4$ generic (random) phase-less measurements are both necessary and suffice to reconstruct N complex-valued unknowns exactly^[23,24]. In the FD-IQI estimation, the conjecture can be interpreted that $K > 8L$ pilot signal blocks (thus, $KL > 8L^2$ symbols in total) is enough to uniquely determine $\bar{\mathbf{h}}$ from ψ . Moreover, the pilot can be a random sequence; this indicates the capability of in-service and/or format-transparent monitoring.

Secondly, the contemporary PR algorithms, such as the Wirtinger flow, allows us to solve the random quadratic system of equations as in (3) nearly as easy as solving linear systems^[25]; the hundreds or thousands of forward and backward Fourier transformations in the classical PR algorithms is not necessary. In this work, we employ a robust and low-complexity PR algorithm based on alternating direction method of multipliers, called PhareADMM^[26].

Finally, it is worth mentioning that the proposed WL PR approach can be further extended to the dual-polarized case, e.g., $\psi := [\psi_{Xk}, \psi_{Yk}]^\top$, $\bar{\mathbf{h}} := [\mathbf{h}_{X+}^\top, \mathbf{h}_{X-}^\top, \delta_X, \mathbf{h}_{Y+}^\top, \mathbf{h}_{Y-}^\top, \delta_Y]^\top$, and $\bar{\mathbf{s}}_k := [\mathbf{s}_{Xk}^\top, \mathbf{s}_{Xk}^H, 1, \mathbf{s}_{Yk}^\top, \mathbf{s}_{Yk}^H, 1]^\top$. It is left for our future work.

Proof-of-Concept Demonstration

Fig. 2 shows the experimental setup. The optical DP-IQ modulator consisted of a 1550.92-nm laser with 100-kHz linewidth, 4-channel 92Gs/s arbitrary waveform generator (AWG), and two LiNO3 Mach-Zehnder IQ modulator. To simulate FD-IQI, 63.25-Gbaud 16QAM signal on the X-polarization was pre-distorted in the digital domain by a (13×2) -tap (i.e., $L = 13$) WL filter $\bar{\mathbf{h}}_{\text{ideal}} := [\mathbf{h}_{\text{ideal}+}^\top, \mathbf{h}_{\text{ideal}-}^\top]^\top \in \mathbb{C}^{26 \times 1}$. The modulator output was amplified, and input to SP-IQM (after PBS) or an IQM based on a standard optical coherent receiver, namely Coh-IQM.

The input powers were +10 dBm and -10 dBm for SP-IQM and Coh-IQM, respectively. SP-IQM consisted of a 70-GHz PD and a 160-GSa/s digital storage oscilloscope (DSO). The +10 dBm input was required due to the lack of transimpedance amplifiers after the PD. The received signal was resampled in the digital domain; as in (3), SP-IQM exploits only every L received samples. The effective sample rate was

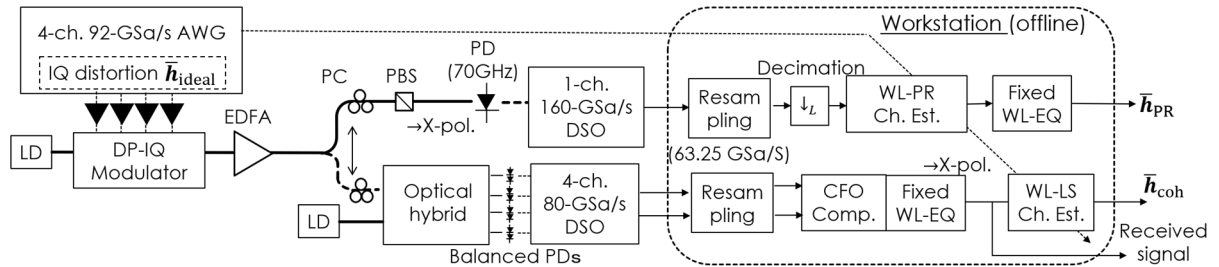


Fig. 2: Experimental Setup for single-pixel IQ monitoring of 63.25-Gbaud 16QAM signal

$63.25/13 \cong 4.86$ GSa/s. Meanwhile, the coherent receiver output was sampled by a 4-channel 80-GSa/s DSO. The random 16QAM sequence of 84,000 symbols long was exploited as pilot (i.e., $84,000/13 \cong 6,400$ samples were processed in SP-IQM). In SP-IQM, FD-IQI was estimated as a (13×2) -tap WL filter $\bar{\mathbf{h}}_{\text{PR}} := [\mathbf{h}_{\text{PR+}}^T, \mathbf{h}_{\text{PR-}}^T]^T$ by PhareADMM with the step size 0.1. The number of the iterations was 100. Here, the bias term δ was omitted here for simplicity. Some results on the joint bias estimation will be reported in our forthcoming publications. In Coh-IQM, the (13×2) -tap filter $\bar{\mathbf{h}}_{\text{coh}} := [\mathbf{h}_{\text{coh+}}^T, \mathbf{h}_{\text{coh-}}^T]^T$ was obtained based on the WL minimum mean-square error (MMSE) criteria^[27]. In each IQM, a fixed WL-MMSE equalizer was employed to mitigate the inherent frequency response and IQI in the transceiver front-end. In Coh-IQM, CFO was removed before the fixed equalizer. Note that, any PR algorithm suffers from global phase ambiguity^[19]. The WL-PR problem also has ambiguity of *phase conjugation*, i.e., $|\bar{\mathbf{h}}| = |\bar{\mathbf{h}}^*|$. However, we are mainly interested in the mismatch between IQ tributaries here and the ambiguities won't be problems in practice.

First, we evaluated the performance of the IQMs for three distinctive IQI patterns. Fig. 3 shows $\bar{\mathbf{h}}_{\text{PR}}$, $\bar{\mathbf{h}}_{\text{coh}}$, and $\bar{\mathbf{h}}_{\text{ideal}}$ in the time and frequency domains for the three cases. Fig. 4 shows the reconstructed (simulated) 16QAM constellations by filtering a random 16QAM

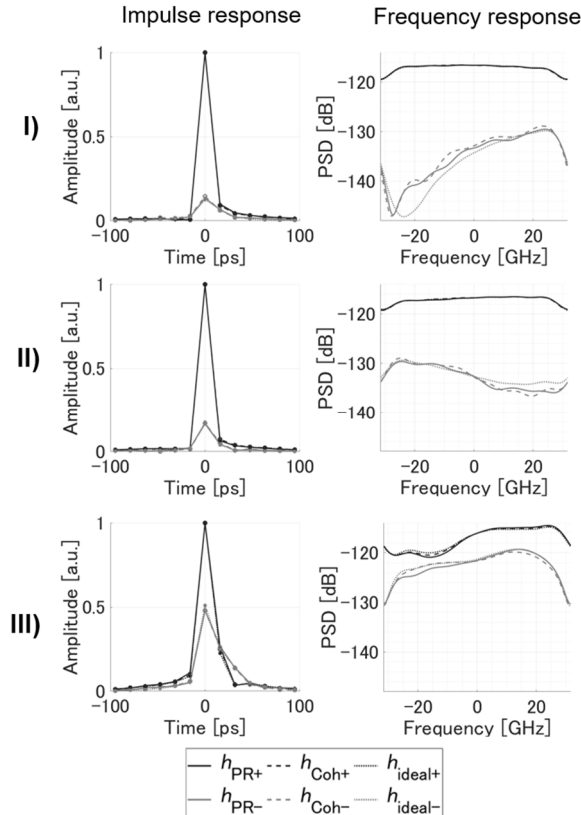


Fig. 3: Estimated impulse responses and frequency responses for 3 distinctive FD-IQI patterns.

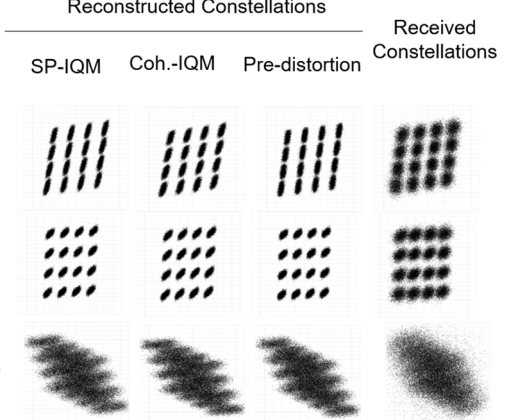


Fig. 4: Received and reconstructed 16QAM constellation maps for 3 distinctive FD-IQI patterns.

sequence with $\bar{\mathbf{h}}_{\text{PR}}$, $\bar{\mathbf{h}}_{\text{coh}}$, and $\bar{\mathbf{h}}_{\text{ideal}}$. The raw received constellations are also shown. As shown in Figs. 3 and 4, the FD-IQIs were successfully estimated via the proposed single-pixel approach. The MSE performance, i.e., $\text{MSE}(\bar{\mathbf{h}}) := E[\|\bar{\mathbf{h}} - \bar{\mathbf{h}}_{\text{ideal}}\|^2 / \|\bar{\mathbf{h}}_{\text{ideal}}\|^2]$, were 1.64×10^{-3} and 1.57×10^{-3} for SP-IQM and Coh-IQM, respectively. Note that, the actual response of the equipment was not considered in $\bar{\mathbf{h}}_{\text{ideal}}$. Meanwhile, $\bar{\mathbf{h}}_{\text{coh}}$ suffered from the residual receiver-side IQI. Thus, all the estimates were biased here. However, their agreement indicated the validity of the proposed PR-based approach.

Next, the statistical performance was evaluated by randomly changing the predistortion filter, i.e., $\mathbf{h}_{\text{ideal+/-}} = \{\mathbf{h}_I \pm (1 + \epsilon)\mathbf{h}_Q e^{j\theta}\}/2$, where $\{\mathbf{h}_I, \mathbf{h}_Q\} \sim \mathcal{N}_c(\mathbf{g}, 0.005\mathbf{I}_{13 \times 13})$ (\mathbf{g} is a raised-cosine filter with roll-off factor 0.2), $\epsilon \sim \mathcal{N}(0, 0.00160)$, and $\theta \sim \mathcal{N}(0, 0.0632)$. We measured the MSE performances over 20 different IQI patterns. The average MSEs were 4.22×10^{-3} and 2.57×10^{-3} for SP-IQM and Coh-IQM, respectively. Though its simpler front-end, SP-IQM achieved the comparable performance to Coh-IQM for various IQI patterns. Interestingly, for some IQI patterns, SP-IQM outperformed Coh-IQM. IQI is known to degrade the CFO estimation performance^[18]; the residual CFO can deteriorate the performance of Coh-IQM. SP-IQM, which is free from the receiver IQI and CFO, also has a potential to be a reference for the initial calibration of coherent receivers.

Conclusions

A low-complexity monitoring of frequency-dependent IQI based on phase retrieval was proposed and experimentally demonstrated for in-service and in-field monitoring of optical higher-order and symbol rate formats.

Acknowledgements

This work was partially supported by the commissioned research by NICT and JSPS KAKENHI Grant Numbers: JP19K04384, Japan.

References

- [1] J. Liang, Y. Fan, Z. Tao, X. Su, and H. Nakashima, "Transceiver Imbalances Compensation and Monitoring by Receiver DSP," *J. Lightwave Technol.* (early access), doi: 10.1109/JLT.2019.2944830. (2019).
- [2] M. S. Faruk and S. J. Savory, "Digital Signal Processing for Coherent Transceivers Employing Multilevel Formats," *J. Lightwave Technol.*, 35(5), 1125–1141 (2017).
- [3] Optical Internetworking Forum (OIF), OIF-CFP2-ACO-01.0, (2016).
- [4] Optical Internetworking Forum (OIF), IA# OIF-400ZR 0.13 Draft. [Online] Available: <https://www.oiforum.com/get/49180>, (2019)
- [5] X. Chen, J. Cho, A. Adamiecki, and P. Winzer, "16384-QAM Transmission at 10 GBD over 25-km SSMF using Polarization-Multiplexed Probabilistic Constellation Shaping," in proc. ECOC2019, Paper PD.3.3 (2019)
- [6] C. R. S. Fludger, T. Duthel, P. Hermann, and T. Kupfer, "Low cost transmitter self-calibration of time delay and frequency response for high baud-rate QAM transceivers," in proc. OFC2017, Paper Th1D.3 (2017)
- [7] Q. Wang, Y. Yue, and J. Anderson, "Detection and compensation of power imbalance, modulation strength, and bias drift in coherent IQ transmitter through digital filter," *Opt. Express* 26(18), 23069–23083 (2018).
- [8] C. Ju, N. Liu, and C. Li, "In-Service Blind Transceiver IQ Imbalance and Skew Monitoring in Long-Haul Non-Dispersion Managed Coherent Optical Systems," *IEEE Access* 7, 150051–150059 (2019).
- [9] G. Khanna, B. Spinnler, S. Calabro, E. De Man, and N. Hanik, "A Robust Adaptive Pre-Distortion Method for Optical Communication Transmitters," *IEEE Photonics Technol. Lett.* 28, 752–755 (2016).
- [10] C. R. S. Fludger and T. Kupfer, "Transmitter Impairment Mitigation and Monitoring for High Baud-Rate, High Order Modulation Systems," in proc. ECOC 2016, Paper Tu.2.A.2 (2016).
- [11] Y. Yue, Q. Wang, and J. Anderson, "Transmitter skew tolerance and spectral efficiency tradeoff in high baud-rate QAM optical communication systems," *Opt. Express* 26(12), 15045–15058 (2018).
- [12] P. Skvortcov, C. Sanchez-Costa, I. Phillips, and W. Forysiak, "Receiver DSP Highly Tolerant to Transmitter IQ Impairments," in proc. OFC2019, Paper Th1D.2 (2019)
- [13] Y. Fan, Y. Jiang, J. Liang, Z. Tao, H. Nakashima, and T. Hoshida, "Transceiver IQ imperfection Monitor by Digital Signal Processing in Coherent Receiver," in proc. OECC/PSC2019, Paper ThC2-1 (2019)
- [14] Q. Zhang, Y. Yang, C. Guo, X. Zhou, Y. Yao, A. P. T. Lau, and C. Lu, "Algorithms for Blind Separation and Estimation of Transmitter and Receiver IQ Imbalances," *J. Lightwave Technol.* 37(10), 2201–2208 (2019).
- [15] Y. Yue, B. Zhang, Q. Wang, R. Lofland, J. O'Neil, and J. Anderson, "Detection and alignment of dual-polarization optical quadrature amplitude transmitter IQ and XY skews using reconfigurable interference," *Opt. Express* 24(6), 6719–6734 (2016).
- [16] Y. Fan, Z. Tao, L. Dou, Y. Zhao, H. Chen, S. Taku, K. Kousuke, T. Hoshida, and J. C. Rasmussen, "Overall Frequency Response Measurement of DSP-based Optical Transmitter Using Built-in Monitor Photodiode," in proc. ECOC2016, Paper Th.2.P2 (2016)
- [17] J. C. M. Diniz, F. Da Ros, E. P. da Silva, R. T. Jones, and D. Zibar, "Optimization of DP-M-QAM Transmitter Using Cooperative Coevolutionary Genetic Algorithm," *J. Lightwave Technol.* 36(12), 2450–2462 (2018).
- [18] X. Dai, X. Li, M. Luo, and S. Yu, "Numerical simulation and experimental demonstration of accurate machine learning aided IQ time-skew and power-imbalance identification for coherent transmitters," *Opt. Express* 27(26), 38367–38381 (2019).
- [19] Y. Shechtman, Y. C. Eldar, O. Cohen, H. N. Chapman, J. Miao, and M. Segev, "Phase Retrieval with Application to Optical Imaging: A contemporary overview," *IEEE Signal Process. Mag.* 32(3), 87–109 (2015).
- [20] L. Anttila, M. Valkama, and M. Renfors, "Frequency-Selective I/Q Mismatch Calibration of Wideband Direct-Conversion Transmitters," *IEEE Trans. Circuits Syst. Express Briefs* 55(4), 359–363 (2008).
- [21] M. Kim, Y. Maruichi, and J. Takada, "Parametric Method of Frequency-Dependent I/Q Imbalance Compensation for Wideband Quadrature Modulator," *IEEE Trans. Microw. Theory Tech.* 61(1), 270–280 (2013).
- [22] Y. Yoshida, T. Umezawa, A. Kanno, and N. Yamamoto, "A Phase-Retrieving Coherent Receiver Based on Two-Dimensional Photodetector Array," *J. Lightwave Technol.* 38(1), 90–100 (2020).
- [23] A. S. Bandeira, J. Cahill, D. G. Mixon, and A. A. Nelson, "Saving phase: Injectivity and stability for phase retrieval," *Appl. Comput. Harmon. Anal.* 37(1), 106–125 (2014).
- [24] A. Conca, D. Edidin, M. Hering, and C. Vinzant, "An algebraic characterization of injectivity in phase retrieval," *Appl. Comput. Harmon. Anal.* 38(2), 346–356 (2015).
- [25] Y. Chen and E. J. Candès, "Solving Random Quadratic Systems of Equations Is Nearly as Easy as Solving Linear Systems," *Communications on Pure and Applied Mathematics* 70(5), 822–883 (2017).
- [26] J. Liang, P. Stoica, Y. Jing, and J. Li, "Phase Retrieval via the Alternating Direction Method of Multipliers," *IEEE Signal Process. Lett.* 25(1), 5–9 (2018).
- [27] T. Adali, P. J. Schreier, and L. L. Scharf, "Complex-Valued Signal Processing: The Proper Way to Deal With Impropriety," *IEEE Trans. Signal Process.* 59(11), 5101–5125 (2011).
- [28] F. Horlin and A. Bourdoux, *Digital compensation for analog front-ends: A new approach to wireless transceiver design* (John Wiley & Sons, 2008).